Durable benefit and change in TCR clonality with nivolumab in a Lynch syndrome–associated glioma

Santiago Cabezas-Camarero(iD), Rebeca Pérez-Alfayate*, Vanesa García-Barberán*, María Carmen Polidura, María Natividad Gómez-Ruiz, Isabel Casado-Fariñas, Issa Ahmad Subhi-Issa, José Carlos Plaza Hernández, Pilar Garre, Isabel Díaz-Millán and Pedro Pérez-Segura

Abstract: Germline replication-repair deficient (gRRD) gliomas are exceptional events, and only a few of them have been treated with immune checkpoint inhibitors (ICIs). Contrary to sporadic gliomas, where ICIs have failed to show any objective benefit, the very few patients with gRRD gliomas treated with ICIs to date seem to benefit from programmed-death-1 (PD-1) inhibitors, such as nivolumab or pembrolizumab, either in terms of durable responses or in terms of survival. T-cell immunohistochemistry (IHC) and T-cell receptor (TCR) repertoire using high-throughput next-generation sequencing (NGS) with the Oncomine TCR-Beta-SR assay (Thermo Fisher Scientific) were analyzed in pre- and post-nivolumab tumor biopsies obtained from a patient with a Lynch syndrome-associated glioma due to a germline pathogenic *hMLH1* mutation. The aim was to describe changes in the T-cell quantity and clonality after treatment with nivolumab to better understand the role of acquired immunity in gRRD gliomas. The patient showed a slow disease progression and overall survival of 10 months since the start of anti-PD-1 therapy with excellent tolerance. A very scant T-cell infiltrate was observed both at initial diagnosis and after four cycles of nivolumab. The drastic change observed in TCR clonality in the post-nivolumab biopsy may be explained by the highly spatial and temporal heterogeneity of glioblastomas. Despite the durable benefit from nivolumab, the scant T-cell infiltrate possibly explains the lack of objective response to anti-PD-1 therapy. The major change in TCR clonality observed after nivolumab possibly reflects the evolving molecular heterogeneity in a highly pre-treated disease. An in-deep review of the available literature regarding the role of ICIs in both sporadic and gRRD gliomas was conducted.

Keywords: glioblastoma, glioma, lynch syndrome, MLH1, nivolumab

Introduction

Lynch syndrome (LS) is an autosomal-dominant inherited disease characterized by germline mutations in mismatch-repair (MMR) genes with an increased risk of colorectal, endometrial, ovarian, and urinary tract cancers. In addition, the occurrence of gliomas is recognized as a rare presentation of LS. The so-called Turcot syndrome refers to those patients with both colorectal cancer (CRC) and primary malignant central nervous system (CNS) tumors secondary to either LS or to familial adenomatous polyposis (APC). MMR-deficient (MMRd) malignancies secondary to LS are microsatellite instability-high (MSI-H) tumors, characterized by a high tumor mutational burden (TMB) that translates into a high neoantigen load that permits an easier and more straightforward recognition by the immune system, which may explain the higher objective responses and durable benefit seen with

Correspondence to:
Santiago Cabezas-Camarero
Medical Oncology Department, Hospital Clínico Universitario San Carlos, Instituto de Investigación Sanitaria San Carlos (IdISSC), Calle Profesor Martin Lagos S/N, 28040, Madrid, Spain.
santiago.cabezas@salud.madrid.org

Rebeca Pérez-Alfayate
Department of Neurosurgery, Instituto de Neurociencias, Hospital Clínico Universitario San Carlos, Madrid, Spain

Vanesa García-Barberán
Molecular Oncology Laboratory, Medical Oncology Department, Hospital Clínico Universitario San Carlos, Instituto de Investigación Sanitaria San Carlos (IdISSC), Madrid, Spain

María Carmen Polidura María Natividad Gómez-Ruiz
Radiology Department, Hospital Clínico Universitario San Carlos, Madrid, Spain

Isabel Casado-Fariñas Issa Ahmad Subhi-Issa José Carlos Plaza Hernández
Pathology Department, Hospital Clínico Universitario San Carlos, Madrid, Spain

Pilar Garre
Molecular Diagnosis Unit, Clinical Chemistry Department, IML, Instituto de Investigación Sanitaria San Carlos (IdISSC), Hospital Clínico Universitario San Carlos, Madrid, Spain

Isabel Díaz-Millán
Research Nurse, Medical Oncology Department, Hospital Clínico Universitario San Carlos, Madrid, Spain

Pedro Pérez-Segura
Medical Oncology Department, Hospital Clínico Universitario San Carlos, Instituto de Investigación Sanitaria San Carlos (IdISSC), Madrid, Spain

*Contributed equally

immune-checkpoint inhibitors (ICIs) in these tumors.[1,2] While ICIs against the programmed-death-1 (PD-1)/programmed death-ligand 1 (PD-L1) axis have not shown efficacy either alone or in combination with bevacizumab or temozolomide in sporadic newly diagnosed or recurrent glioblastoma (GB) (Table 1), a few reported cases of GB associated with germline replication-repair defects (gRRDs) have shown tumor responses to anti-PD-1 agents.[3–20] Brilliant responses to these agents have been reported in biallelic mismatch-repair deficiency syndrome (BMMRDS) characterized by the appearance of CNS tumors and hematological cancers at early ages. Benefit from ICIs has also been reported in LS-associated GB (Table 2). Contrary to these gRRD-driven tumors, most patients with somatic replication-repair deficient (RRD) high-grade gliomas (HGG) have not been shown to derive benefit from ICIs[17,21–23] (Table 2). We report the case of a patient with LS due to an *MLH1* germline mutation presenting with a isocitrate dehydrogenase (IDH) wild-type GB as per the 2021, 5th edition of the World Health Organization (WHO) classification of CNS tumors (it had originally been classified as a grade II astrocytoma as per the 2007, 4th edition of the WHO classification of CNS tumors).[24,25] The patient received five lines of therapy before being treated with the anti-PD-1 nivolumab, showing a slow radiological progression. To describe the changes in T-cell presence and clonality induced by treatment, T-cell immunohistochemistry (IHC) and T-cell receptor (TCR) repertoire were analyzed. When comparing the biopsy from initial diagnosis and that performed after progression with nivolumab, no gross changes in the presence of T cells occurred, but a change in TCR clonality was observed. To our knowledge, this is the fifth case reported in the literature of an LS-associated glioma treated with ICIs.

Materials and methods

Ethical considerations
This study was approved by the Institutional Review Board of Hospital Clínico Universitario San Carlos, in accordance with the principles outlined in the 'World Medical Association Declaration of Helsinki'. A signed informed consent form was obtained from the patient prior to study participation, allowing for publication of this case report, including any accompanying data and images.

Sample collection and processing
The current study used tumor samples from 2013 and 2019. In 2013, a partial tumor resection was undertaken. In 2019, a neuronavigation-assisted tumor biopsy was undertaken. Both tumor samples were formalin-fixed and paraffin-embedded (FFPE).

Immunohistochemistry
IDH1-R132H antibody (clone H09; dilution 1:20), and anti-CD4 (clone 4B12; dilution 1:40), anti-CD8 (clone C8/144B; dilution 1:50), anti-PD-L1 (clone 22C3; dilution 1:50), MLH1 (clone ES05; dilution 1:100), MSH2 (clone FE11; dilution 1:150), MSH6 (clone EP49; dilution 1:50), and PMS2 (clone EP51; dilution 1:50) antibodies (all from Dako North America, Carpintería, CA, USA) were used for studying IDH1 status and T-cell and MMR protein expression by IHC. Positive PD-L1 expression in tumor cells was defined as a membranous staining in at least 1% of tumor cells.[11]

DNA extraction
Tumor DNA was obtained from 4 to 8 sections of paraffin-embedded tumor tissue (tumor region was selected by a pathologist) using the 'QIAamp DNA FFPE Kit GenRead' kit (QIAGEN, Germantown, MD, USA). This kit removes the cytosine deamination artifacts, minimizing the risk of false single nucleotide polymorphism (SNP) calls. Tumor DNA was quantified using a QUBIT 3.0 fluorometer instrument (Thermo Fisher Scientific, Waltham, Massachusetts, USA).

Next-generation sequencing study of IDH1 and IDH2 mutations in tumor tissue
Next-generation sequencing (NGS)-based panel was designed using DesignStudio tool (Illumina, Inc., USA) to optimize target region sequencing coverage. The whole exonic region of IDH1 and IDH2 was sequenced, following the manufacturer's instructions as previously described.[26] DNA from FFPE tumor samples was quantified using Qubit dsDNA HS Assay (Thermo Fisher Scientific, Waltham, Massachusetts, USA) and 50–150 ng was used for mutational analysis by AmpliSeq methodology (Illumina, Inc., USA). AmpliSeq Library PLUS was used for library preparation (Illumina, Inc., USA), according to the manufacturer's protocol. After amplification of target regions, primer dimers and partially digest

Table 1. Studies with ICIs in patients with sporadic HGG.

Study	N, tumor type (type of study)	Design	Biomarkers	GCs at IO start	Response	PFS	OS	Toxicity
Reiss et al.[3]	N = 25 rHGG (RS)	Pembro in rHGG	–	14/25 (56%)	2 PR, 5 SD, 17 PD	1.4 m 3-m PFS: 12%	4 m 6-m OS: 28%	G3–4 AEs: 24%
Cloughesy et al.[5]	N = 35 rGBM (Phase II)	Neoadj + adj Pembro: N = 17 Adj Pembro: N = 19	-Higher ↑ IFN-γ and T-cell activation IRG in the neoadj versus adj group. -Lower ↑ cell cycle / cancer proliferation RG in the neoadj versus adj group. -↑ of expanded T-cell clones in the neoadj group pre- versus post-surgery in tumor and PB.	14/32 (44%)	–	Neoadj versus adj: 3.3 m versus 2.4, HR 0.43, p = 0.03	Neoadj versus adj: 13.2 m versus 6.3, HR 0.35, p = 0.03	No surgery delays G3–4 Aes neoadj: 67% G3–4 Aes adj: 47%
Zhao et al.[6]	N = 66 rGBM (RS)	Anti-PD-1 (Pembro or Nivo) in rGBM	-PTEN mut R versus NR: 23% versus 72% (p = 0.006) -MAPK mut R versus NR: 31% versus 3% (p = 0.019) -Different clonal tumor evolution in R versus NR -Higher ↑ in B-cell and T-cell clonal diversity in NR versus R -More baseline CD68 + HLA-DR macrophages in PTEN mut versus wt -↑ in CD3+ and CD8+ T-cells post-IO in PTEN wt	–	13/42 (31%)	–	R versus NR: 14.3 versus 10.1 m (p = 0.0081)	–
Schalper et al.[7]	N = 27 rGBM N = 3 pGBM (Phase II)	Neoadj + adj Nivo	-Pre- to post-Nivo: ↑ IRG, ↑ TCR clones, clonotypes and diversity -High versus Low TCR diversity increased OS: 125 versus 84 days.	–	–	4.1 m	7.3 m	irTRAEs G2: ALT ↑, hyperthyroidism, Other AEs: two intratumoral bleeding pre-SX
Sahebjam et al.[8]	N = 32 rHGG (Phase II)	Pembro + Bev + HFSRT Bev-N: N = 24 Bev-R: N = 8	CPS ≥ 1: 6/26 (23%) TMB-High: 1/16 (6.25%)	Bev-N: 21% Bev-R: 25%	Bev-N: 83.3% Bev-R: 62.5%	Bev-N versus Bev-R: 7.9 versus 6.5 m	Bev-N versus Bev-R: 13.4 versus 9.3 m	G3–4 AEs: 37.5%
De Groot et al.[9]	N = 15 rGBM (Phase II)	Pembro × 2 → SX → Adj Pembro	-CD68 + macrophages: *Most abundant immune population (11/18 immune clusters) *Enriched in immunosuppressive biomarkers *Frequent enrichment in CD163 immunosuppressive macrophages -Very low frequency of T effector cells -No change in PB immune subsets after Pembro	–	3/15 (20%)	4.5 m 6-m PFS: 40%	20 m 1-y OS: 63%	TRAEs: 0%

(Continued)

Table 1. (Continued)

Study	N, tumor type (type of study)	Design	Biomarkers	GCs at IO start	Response	PFS	OS	Toxicity
Nayak et al.[10]	N=87 Bev-N rGBM [Phase II]	Pembro + Bev (A): N=50 Pembro (B): N=30 Primary Endp: 6-m PFS	PD-L1 ≥ 1 (A versus B): 44% versus 30% TIL density (A versus B): *Low: 50% versus 33% *High: 40% versus 50% *No correlation with efficacy GEP (A versus B): *Low (72% versus 56.7%): predict rapid PD with Pembro *High (8% versus 20%)	A versus B: 24% versus 23.3%	ORR (A versus B): 20% versus 0% Responses were durable	6-m PFS (A versus B): 26% versus 6.7% PFS (A versus B): 4.1 versus 1.4 m (p=0.026)	OS (A versus B): 8.8 versus 10.3 m (p=0.87) Worse OS with baseline GCs	G3 TRAEs (A versus B): 32% versus 13%
Reardon et al.[12]	N=26 PD-L1+rGBM [Phase I; Keynote-028]	Pembro	PD-L1 ≥ 1: 26/26 (100%) GEP score (N=18): very low MSI-H: 0/26 (0%)	27%	ORR: 2/26 (8%)	PFS: 2.8 m 6-m PFS: 37.7%	OS: 13.1 m 12-m OS: 58%	G3-4 TRAEs: 19.2%
Omuro et al.[4]	N=40 rGBM [Phase I; Checkmate-143]	Nivo3: N=10, Nivo1 + Ipi3: N=10 Nivo3 + Ipi1: N=20	PD-L1 ≥ 1%: 68% PD-L1 ≥ 10%: 27%	Nivo3: 20%, Nivo1 + Ipi3: 40% Nivo3 + Ipi1: 30%	ORR: 3/40 (7.5%; Nivo3: N=1; Nivo3-Ipi1: N=2) SD ≥ 12 week: 8/40	PFS: Nivo3: 1.9 m, Nivo1 + Ipi3: 1.5 m Nivo3 + Ipi1: 2.1 m	OS: Nivo3: 10.4 m Nivo1 + Ipi3: 9.2 m Nivo3 + Ipi1: 7.3 m	G3-4 TRAEs: Nivo3: 0 Nivo1 + Ipi3: 90% Nivo3 + Ipi1: 30%
Reardon et al.[11]	N=369 rGBM [Phase III; Checkmate-143]	Nivo versus Bev (1:1)	Nivo versus Bev: PD-L1 ≥ 1: 26.1% versus 18.9%	GCs Nivo versus Bev: 39.7% versus 42.7%	ORR Nivo versus Bev: 7.8% versus 23.1%	Nivo versus Bev: *PFS: 1.5 versus 3.5 m, HR 1.97, p<0.001 *6-m PFS: 15.7% versus 29.6%	Nivo versus Bev: *OS: 9.8 versus 10 m, HR 1.04, p=0.76 *12-m OS: 42% versus 42% *No-GCs + MGMTmet: 17 versus 10.1 m, HR 0.58 *GCs + MGMTunmet: 5.6 versus 8.3 m.	G3-4 TRAEs (Nivo versus Bev): 18.1% versus 15.2%

Adj, adjuvant; AEs, adverse events; Bev, bevacizumab; Bev-N, bevacizumab-naïve; Bev-R, bevacizumab-resistant; GBM, glioblastoma; GCs, glucocorticoids; GEP, T-cell-inflamed gene expression profile; HFSRT, hypofractionated stereotactic radiotherapy; HGG, high-grade glioma; HR, hazard ratio; IO, immunotherapy; Ipi, ipilimumab; IRG, immune-regulatory genes; irTRAEs, immune-related TRAEs; MGMT, O6-Methylguanine-DNA Methyltransferase; MGMTmet, MGMT methylated; MGMTunmet, MGMT unmethylated; MSI-H, microsatellite instability-high; mut, mutant; N, number of patients; Neoadj, neoadjuvant; Nivo, nivolumab; ORR, objective response rate; OS, overall survival; PB, peripheral blood; PD, progressive disease; Pembro, pembrolizumab; pGBM, primary GBM; PFS, progression-free survival; rGBM, recurrent glioblastoma; rHGG, recurrent HGG; RS, retrospective series; SD, stable disease; TCR, T-cell receptor; TILs, tumor-infiltrating lymphocytes; TMB, tumor mutational burden; TRAEs, treatment-related adverse events; wt, wild-type; (–), not available.

Table 2. Glioma cases treated with ICIs and harboring germline or somatic mutations in replication-repair genes.

gRRD gliomas

Authors	Age, location, histology	Familial syndrome (germline mutation)	Other disease markers	Additional somatic alterations	Pre-IO treatment	IO agent	Response	Survival	Toxicity
Bouffet et al.[13]	6 years, female, Left parietal MGMT-unmeth GBM	bMMRD (biallelic PMS2 deficiency)	Café-au-lait spots	TP53-mut, POLE-mut, high TMB ('ultra-mutant'), high NAL	SX → RT (59.4 Gy) → PD 3 m post-RT	Nivo	Initial PsPD → PR after sixth cycle	Alive and back to school 9 m post-nivo	Seizures 1 week after first and second cycle, HypoNa+ after second cycle
	3.5 years, male, right fronto-parietal MGMT-unmeth GBM	bMMRD (biallelic PMS2 deficiency)	Café-au-lait spots	TP53-mut, POLE-mut, high TMB ('ultra-mutant'), high NAL	SX → RT (59.4 Gy) → PD 10 m post-RT	Nivo	Initial PsPD → PR after fourth cycle	Alive and back to school 5 m post-Nivo	Seizures 11 days after first cycle
Pavelka et al.[16]	Adolescent, GBM	bMMRD (biallelic PMS2 deficiency)	Prior CRC	High TMB	–	Autologous DCs vaccine + Nivo + RT + TMZ	CR	AWOD 21 m after treatment	–
Sherman et al.[19]	57 years, female, left occipital IDH-WT, MGMT-unmeth GBM	LS (–)	Prior CRC (10 years earlier)	MSI-H, High TMB	SX → RT + TMZ → TTF × 14 m	Relapse 3-year post-diagnosis (18-m post-TTF) → SX → Nivo + RT (45 Gy in 25 fx) → Nivo	CR	AWOD 20 m after Nivo start	G2 neutropenia
Anghileri et al.[18]	33 years, female, left frontal GBM	LS (MSH2)	Colonic adenoma with HGD, family history compatible with LS	MSI-H, high TMB, abundant CD8+ TILs	SX → RT + TMZ → TMZ × 6 cycles	Relapse 13 months after diagnosis → Rescue SX (complete resection) → starts adjuvant Nivo	–	AWOD 5 years after starting Nivo	Anemia
AlHarbi et al.[15]	5 years, female, left fronto-parietal lobe GBM with PNET features	bMMRD (biallelic MSH6 deficiency)	Café-au-lait spots, mild facial dysmorphism. Brother died of T-cell lymphoma at 8 years of age	PD-L1-	SX → RT + TMZ → TMZ × 3 cycles → PD with spinal leptomeningeal disease	Nivo × 18 cycles	PR after 6th and 18th cycles	AWD 10 m after starting Nivo	None
Johanns et al.[14]	31 years, male, Left fronto-temporal GBM with PNET features	POLE deficiency syndrome	Personal and family history of colonic polyposis	All three surgical specimens showed high TMB (hypermutant) and high-quality NAL. Primary tumor: 'classical' molecular subtype. Spinal metastases: 'mesenchymal' molecular subtype	SX → RT + TMZ → TMZ × 1 cycle	C7-T2 intradural extramedullary relapse ('drop metastasis') → SX → RT C5-T3 (50.4 Gy) → Pembro × 2 cycles → T7-T8 PD → SX (GBM with inflammatory changes) → Pembro + RT T6-L4 (45 Gy) → Pembro	PR in brain enhancing lesions after 13 weeks of Pembro. PD at spinal intradural metastases with inflammatory changes in surgical specimens after Pembro (increase in TILs and increase in IR gene expression)	Alive 4 m after starting Pembro	–

(Continued)

Table 2. (Continued)

gRRD gliomas

Authors	Age, location, histology	Familial syndrome (germline mutation)	Other disease markers	Additional somatic alterations	Pre-IO treatment	IO agent	Response	Survival	Toxicity
Kamiya-Matsuoka et al.[17]	GBM	LS (MSH2)	–	–	–	Pembro	SD 12m after starting Pembro	AWD 12m after starting Pembro	–
Thomsen et al.[20]	17 years, male, GBM	LS (MSH2)	Family history of CRC, SGC, uterine, bladder, and breast cancers	MSI-H High TMB (40 muts/Mb) Somatic muts: IDH, ATRX, TP53, MSH2	SX (STR) → RT (54 Gy) + TMZ Pembro × 2 → SX (GTR) → Ady Pembro × 2 → PD	Pembro	20% necrosis and increase in TILs in surgical specimens after Pembro	Exitus 12m after DX	–
Current case	GBM	LS (MLH1)	Family history of CRC	Scant TILs presence pre- and post-nivo. Change in TCR clonality post-nivo	TMZ × 12 cycles → SX → RT (60 Gy) → FTM × 3 m → BEV × 27 cycles → WandS × 12 m → BEV × 13 cycles	Nivo	PD after five cycles of Nivo	DWD 9m after starting Nivo	Atoxic

Somatic replication-repair-deficient gliomas

Author	N (histology)	Somatic alteration	Other markers	IO agent	Response	Survival
Ahmad et al.[21]	N = 4 with rGliomas (1 IDHwt GBM, 1 IDHmut AA, 1 IDHmut AOD, 1 grade-II OD)	MSH6 mutant (N = 4), MLH1 mutant (N = 1)	High TMB (N = 3)	>2-line Pembro (N = 3), >2-line Nivo (N = 1)	Pembro: PD (N = 3) Nivo: PD (N = 1)	Pembro: Pt 1 (GIII oligo): PFS 9 week, OS 20 m; Pt 2 (GBM): PFS 12-week, OS 11 m; Pt 3 (GIII astrol): PFS 12 week, OS + 7 m. Nivo: Pt 1 (PFS: 12-week, OS 11 m)
Lombardi et al.[22]	N = 13/310 were IHC MMRd rHGG (8 IDHwt GBM, 3 IDHmut AA, 1 IDHwt AA, 1 IDHmut AOD)	IHC MMR: *MSH2(–): N = 9 *MSH6(–): N = 8 *MLH1(–): N = 2 *PMS2(–): N = 2 MMR gene mutation: *MSH6: N = 1	PD-L1 + (TPS): 0/13 TMB > 10 muts/Mb: 6/12	Pembro	SD 4/13 PD: 9/13 DCR: 31% DoR SD: 7.7m	PFS: 2.2m OS: 5.6 m 12-m OS: 38%
Kamiya-Matsuoka et al.[17]	N = 30/312 were HmGBM N = 9/30 HmGBM received IO (Primary HmGBM: N = 5; Post-TMZ HmGBM N = 4) (N = 7 MMRd, N = 2 POL-mut).	sMMRd: N = 8 gMMRd (MSH2): N = 1	–	ICI or Cellular therapy (T cells or NK cells). At recurrence N = 8, At primary diax N = 1.	–	PFS (sMMRd): 72 days *6-m PFS: 0% *PFS HmGBM post-TMZ: 51 days (ICI), 41 days (T cells), 175 days (NK cells) *PFS primary HmGBM: 96 days PFS (gMMRd): 12 m (pembro)

AA, anaplastic astrocytoma; AOD, anaplastic oligodendroglioma; AWD, alive with disease; AWOD, alive without disease; Bev, bevacizumab; bMMRD, biallelic mismatch-repair deficiency syndrome; CR, complete response; CRC, colorectal cancer; Diax, diagnosis; DWD, dead with disease; FTM, fotemustine; GBM, glioblastoma multiforme; gMMRd, germline MMRd; HmGBM, hypermutated GBM; HGD, high-grade dysplasia; ICI, immune checkpoint inhibitors; IDH, isocitrate dehydrogenase; IDHmut, IDH mutant; IDHwt, IDH wild-type; IHC, immunohistochemistry; IO, immunotherapy; LS, Lynch syndrome; MMRd, mismatch-repair deficient; MSI-H, microsatellite instability-high; Mut, mutant; gMMRd, germline MMRd; N, number of patients; NAL, neoantigen load; Nivo, nivolumab; OD, oligodendroglioma; OS, overall survival; PsPD, pseudoprogressive disease; Pembro, pembrolizumab; PFS, progression-free survival; PR, partial response; rGliomas; recurrent gliomas; RT, radiotherapy; SD, stable disease; sMMRd, somatic MMRd; SX, surgery; TMB, tumor mutational burden; TMZ, temozolomide; W&S, wait and see; (–), not available.

amplicons were digested, and unique combination of index adapters was ligated (AmpliSeq CD Indexes). A second amplification of libraries was performed. Quantity and quality of libraries were checked by Agilent High Sensitivity DNA Kit in an Agilent 2100 Bioanalyzer instrument (Agilent Technologies, Santa Clara, CA, USA). Libraries were diluted to the final loading concentration (7.5–8 pM) and denatured with NaOH for bridge clonal amplification and paired-end sequencing using MiSeq Reagent kit v2 (300 cycles) in a MiSeq instrument (Illumina, Inc., USA). Illumina MiSeq device version 3.1.0.13 (Illumina, Inc., USA) provides alignment (BAM) and variant calling files (vcf). The VariantStudio software (Illumina, Inc., USA) was used to annotate vcf, identifying and classifying the detected genetic variants.

TCR repertoire analysis

The Oncomine TCR-Beta-SR assay (Thermo Fisher Scientific, Waltham, Massachusetts, USA) was used for performing high-throughput NGS to analyze the nucleotide sequence of the CDR3 region coding for the T-cell receptor beta (TCRβ) chain, made up of variable (V), diversity (D), joining (J) (VDJ) and constant regions, following the manufacturer's instructions.[27] In brief, after isolating and quantifying the DNA, amplicons were obtained after amplification from 100 ng of DNA, then were partially digested and ligated with barcode adapters (Ion Torrent Dual Barcode Kit, Thermo Fisher Scientific, Waltham, Massachusetts, USA) to generate barcoded libraries. Amplification of the purified libraries was performed (five cycles of amplification). Libraries were quantified using Ion Library TaqMan Quantitation Kit and diluted to 25 pM concentration. Libraries were combined to be loaded on an Ion 540 chip using the Ion Chef Instrument and sequenced in the Ion GeneStudio S5 System (Thermo Fisher Scientific, Waltham, Massachusetts, USA). Data analysis was performed using Ion Reporter Software. After removing low-quality, off-target, and error-containing reads from the analysis, VDJ rearrangements were reported, followed by a secondary analysis of the TCRβ repertoire.

MLH1 germline testing

Germline DNA was obtained from peripheral blood leukocytes, and Sanger sequencing was performed in a Applied Biosystems ABI 3130 automated sequencer (Applied Biosystems, Foster City, CA, USA) to confirm the *hMLH1* mutation NM_000249:c.1865 T>A; p.(L622H) previously identified in the index family case. Carrier status of our patient was confirmed in peripheral blood from two different blood draws obtained 1 week apart from each other.

Case report

A 34-year-old man, smoker of 40 cigarettes per day, and with grade II obesity, presented to the Emergency Room in August 2012 with an absence of epileptic crisis followed by conjugate gaze deviation and orofacial automatisms, being started on levetiracetam 500 mg/q2wk, with no new episodes. Computed tomography (CT) scan showed a left temporal lobe mass suggesting a low-grade glioma. Brain magnetic resonance imaging (MRI) in September 2012 showed an infiltrating nonenhancing, T1-isointense, T2-hyperintense, and normally perfused (VSCr) left temporal lobe mass invading the cortex and white matter of the parahippocampal convolution, amygdala, and the fusiform and inferior temporal gyruses, compatible with a low-grade diffuse astrocytoma. The tumor mass caused a slight mass effect over the left mesencephalon and minor obliteration of the ipsilateral cisterna ambiens. A repeated brain MRI performed 3 months later showed no apparent changes. In January 2013, a neuronavigation-assisted tumor biopsy was performed confirming the diagnosis of an IDH1-R132H wild-type, low-grade astrocytoma of the left temporal lobe. Sequencing of IDH1 and IDH2 mutations by NGS confirmed the IDH wild-type nature of the tumor. Thereby, it would correspond to an IDH wild-type GB as per the current edition (5th Ed.; 2021) of the WHO Classification of CNS Tumors. The patient informed that his 65-year-old paternal uncle diagnosed with a CRC when he was at the age of 35 years, had been diagnosed of LS after a germline test revealed an *hMLH1* pathogenic mutation NM_000249: c.1865 T>A; p.(L622H). The patient's father, a second paternal uncle and his paternal grandfather, had died from CRC at ages 41, 28, and 50 years, respectively. No other cases of gliomas had been reported in the patient's family. The patient's older brother had undergone a right hemicolectomy due to a 4-cm polyp with high-grade dysplasia at the age of 42 years. He had two 35- and 39-year-old male brothers and two 34-year-old twin sisters, and three small children all of them without any history of cancer. The patient underwent germline genetic testing that confirmed the carrier status of the pathogenic

hMLH1 mutation previously detected in his paternal uncle (Figure 1). Treatment with temozolomide 150–200 mg/m²/days 1–5 in 28-day cycles was administered for 12 months with good tolerance, showing stable disease as best response. In January 2014, a partial resection was performed due to tumor progression, with pathology informing of a grade III IDH wild-type astrocytoma as per 4th edition of the WHO classification of CNS tumors from 2007, corresponding to an IDH wild-type GB as per the current 5th edition.[24,25] Subsequently, the patient received IMRT-based radiotherapy over the tumor mass and safety margins for a total of 60 Gy in 30 fractions (2 Gy per fraction) with good tolerance. Close follow-up ensued until a new brain MRI in February 2015 showed tumor progression. Treatment with fotemustine 80 mg/m²/q2wk was started receiving five cycles but showing a marked tumor progression

with clinical deterioration (left hemianopsia, gait instability, and headache) in May 2015. Treatment with bevacizumab 10 mg/kg/q2wk (25 mg/ml solution) was then started 1 month after the last dose of fotemustine. One week after the first cycle, however, the patient was admitted to the Emergency Room due to the absence crisis and aphasia. The patient was diagnosed with a non-convulsive status epilepticus and transferred to the neurology department where corticosteroids and antiepileptic therapy reverted the episode. Three weeks later, however, treatment with bevacizumab was restarted with no new epileptic episodes and progressive improvement of aphasia and cognitive performance. Brain MRI performed in July 2015, 6 weeks after the first bevacizumab dose, showed a notable radiological improvement, with a complete or near-complete response that kept improving on MRI performed 3 months later, in October
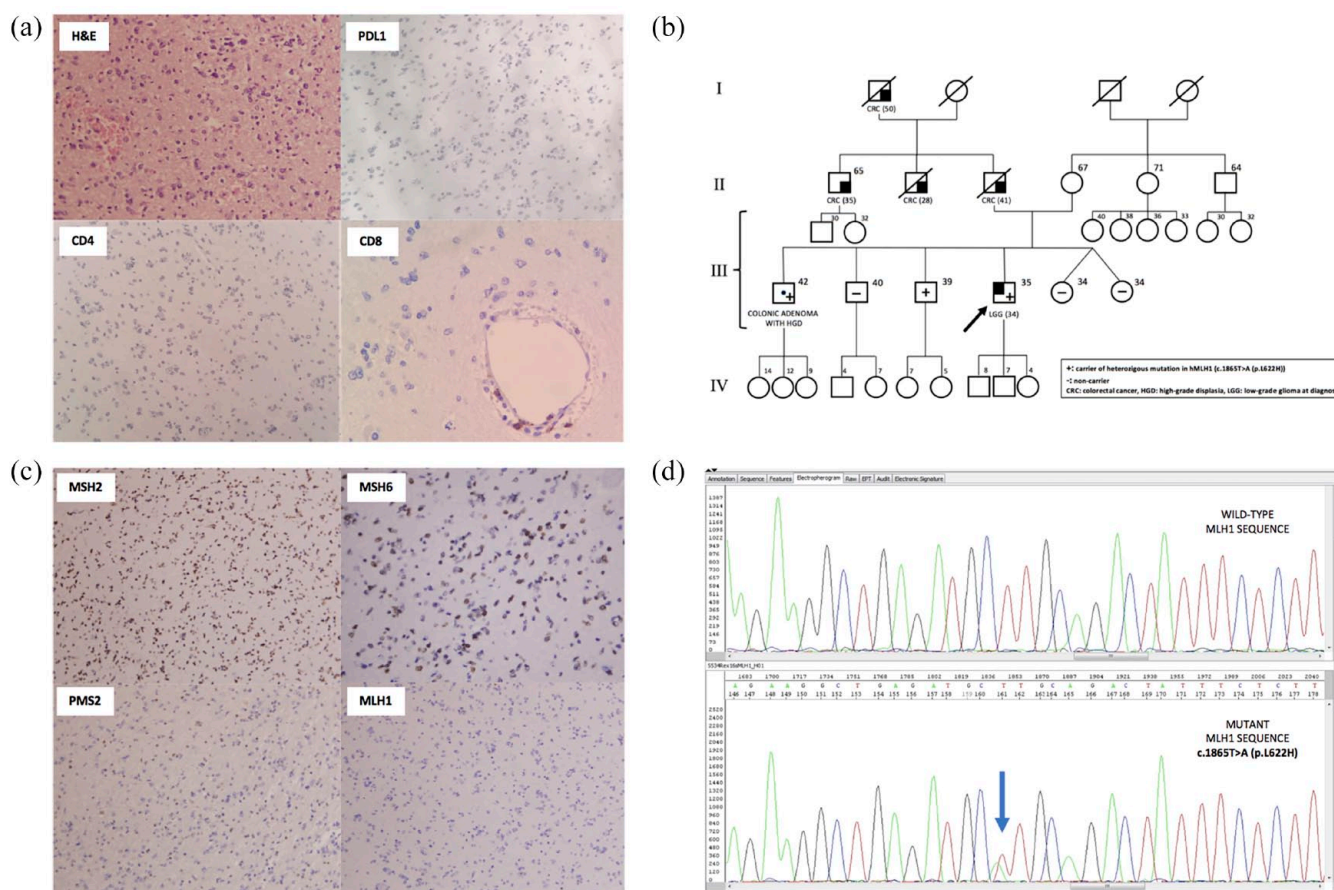

Figure 1. (a) H&E, PD-L1 expression, and T-cell populations in the 2014 tumor biopsy. H&E shows a low-grade glioma, PD-L1 negative, T-CD4 negative and with scant perivascular T CD8+ cells. (b) Pedigree depicting the cancer history of the patient's family, reflecting an autosomal dominant pattern of inheritance. (c) Mismatch-repair protein IHC shows preserved expression of MSH2 and MSH6, partial PMS2 expression and complete lack of expression of MLH1. (d) Sanger sequence of the patient's peripheral blood lymphocytes demonstrating a pathogenic MLH1 mutation [c.1865 T > A (p.L622 H)].
CRC, colorectal cancer; HGD, high-grade dysplasia; LGG, low-grade glioma; (+), mutation carrier; (−), noncarrier.

2015. The patient received a total of 27 bevacizumab cycles until February 2017, when, due to the excellent radiological response, treatment was stopped and a 'wait and see (W&S)' strategy was started. Close follow-up with MRI every 3 months ensued until April 2018, when tumor progression without clinical deterioration occurred. Treatment with bevacizumab was restarted with slow tumor progression and progressive clinical deterioration (worsening of aphasia and gait instability) after 13 cycles, the last one administered in early November 2018. Due to the absence of standard therapeutic options, and the diagnosis of LS due to a germline *hMLH1* mutation NM_000249: c.1865 T>A; p.(L622 H), treatment with the anti-PD-1 agent nivolumab (240 mg/15 days IV; 10 mg/ml solution) *via* a compassionate use authorization was started, 3 weeks after the last bevacizumab dose. MSI status and TMB analyses were not performed due to the lack of remanent sample. After four cycles, MRI performed in February 2019 showed tumor progression. Because of the doubts regarding a potential tumor pseudoprogression secondary to an immune-mediated effect induced by nivolumab, consent was obtained from the patient to perform a neuronavigation-assisted tumor biopsy, informed as an IDH wild-type GB with a scant immune cell infiltrate, thereby confirming tumor progression. Given the clinical stability and good tolerance, the patient received five additional cycles of nivolumab until May 2019, when an overt clinical and radiological progression occurred. A new line with irinotecan (125 mg/m^2/15 days IV) combined with bevacizumab (10 mg/kg/15 days; 25 mg/ml solution) was started 3 weeks after the last dose of nivolumab. Due to toxicity (grade III asthenia, and grade II diarrhea), however, treatment was permanently discontinued after one single cycle administered in June 2019, and the patient was transferred to hospice for end-of-life care where he died 3 months later (Figure 2).

Results

T-cell and PD-L1 IHC

Biopsies from initial diagnosis in 2013 and after four cycles of nivolumab in 2019 showed a scant immune T-cell infiltration predominantly consisting of perivascular T-CD8+ cells with no apparent changes between the 2013 and 2019 biopsies (Figure 1). Likewise, PD-L1 expression was absent in both the 2013 and 2019 tumor specimens (The 2019 biopsy microphotographs are not shown due to inaccessibility to the slides at the time of writing this article and lack of additional material to repeat the IHC study).

MMR proteins IHC and germline genetic testing

IHC of the tumor biopsy from initial diagnosis showed preserved expression of MSH2 and MSH6, with lack of expression of MLH1 and PMS2 as constituents of the *hMutLα* complex (Figure 1).[28]

Germline testing for *hMLH1* mutation NM_000249:c.1865 T>A; p.(L622H) confirmed the carrier status of the patient (Figure 1).

TCR repertoire analysis

The number of TCR clones detected in the 2013 and 2019 biopsies was 26 and 21, respectively. Both Shannon diversity and TCR evenness showed high and comparable values in the 2013 and 2019 biopsies, indicating the good quality of the samples for the analysis. Only one TCR clone was coincident between the two biopsies (V-gene: TRBV12-3, J-gene: TRBJ1-5, CDR3 nucleotide: GCCAGCAGTATTAATTATAGCAAT CAGCCCCAGCAT, CDR3 amino acid: AS SINYSNQPQH), although with a higher frequency in the 2019 compared with 2013 specimen (2013 *versus* 2019 clone frequency: 0.0000006201% *versus* 0.0000179%) (Table 3, Figure 3, and Supplementary Table).

Discussion

Our case is notable for constituting a rare presentation of LS, that is, the development of an IDH wild-type GB in a patient harboring a germline *MLH1* mutation. *MLH1*-driven LS is an autosomal dominant disease characterized by a 40–60% risk of CRC, a 2–12% risk of urinary tract cancer, and, in females, a 30–50% risk of endometrial cancer, and a 5–15% risk of ovarian cancer. Rarely (<2%), patients may develop glial tumors.[29,30] LS is associated with MMR defects leading to MSI, and thereby to hypermutant cancers with a high neoantigen load, which make these tumors easily recognizable by the immune system, and specifically by T cells.[31] This explains why LS-associated cancers show a high objective response rate (ORR) when treated with immunotherapy. While ORR to anti-PD-1 agents alone or in combination with anti-CTLA4 agents in metastatic CRC range from 30% to 60%, only a few cases of LS-associated
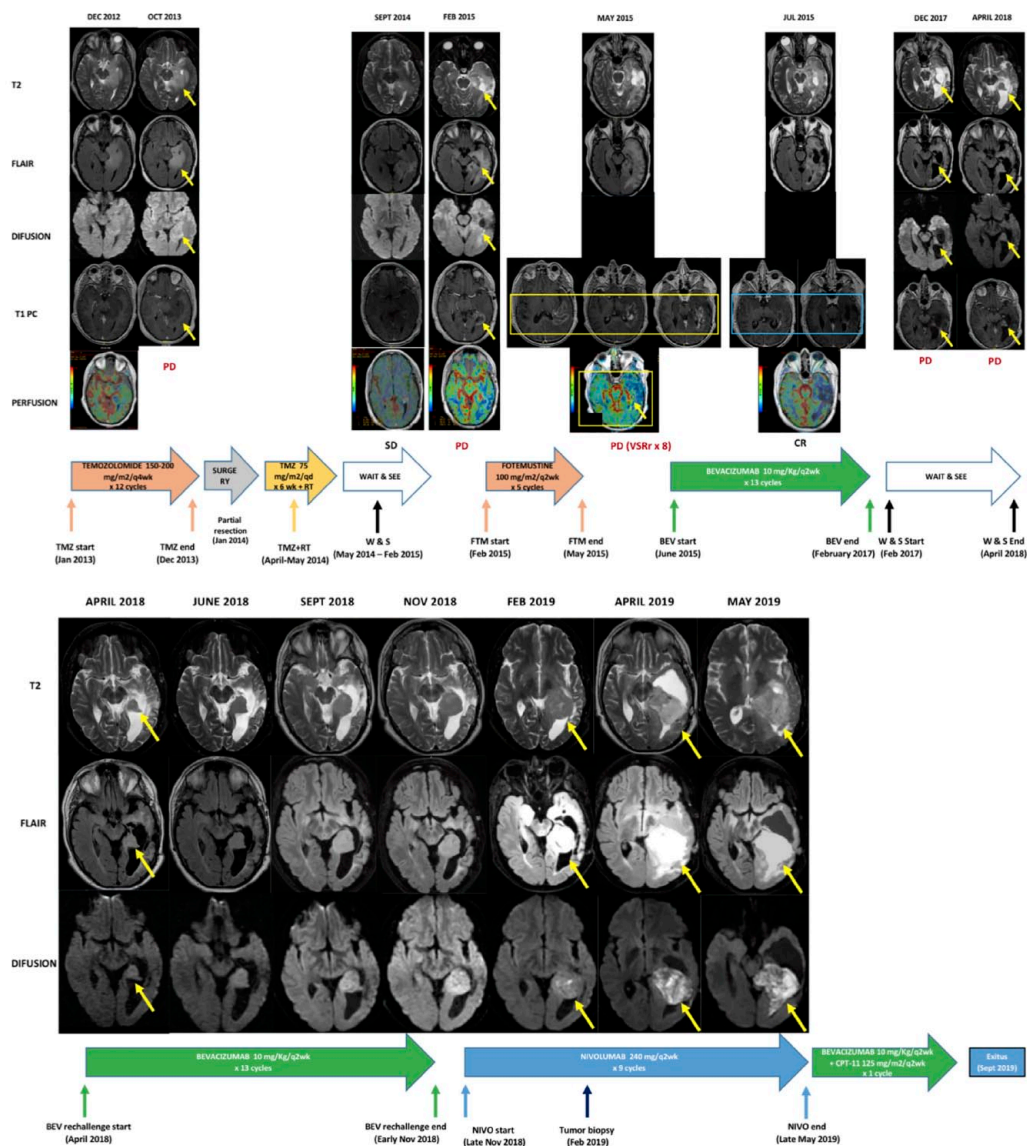
Figure 2. MRI tumor evolution from initial diagnosis until the end of therapy.

Upper row: A large nonenhancing glioma in the left temporal lobe is seen in the MRI from December 2012. A biopsy informed of a grade-II IDH wild-type astrocytoma (according to WHO 2007 4th edition that corresponds to an IDH wild-type GB according to WHO 2021 5th edition classification of CNS tumors) and treatment with single-agent temozolomide was administered for 12 months until PD occurred in January 2014. A partial tumor resection was made followed by adjuvant RT between April and May 2014. A W&S strategy started until February 2015 when due to PD, treatment with FTM was administered between February and May 2015, suffering PD.

Treatment with Bevacizumab 10 mg/kg/q2wk was started in June 2015, experiencing a rapid and complete/near-complete tumor response after only four cycles that was maintained until February 2017, when a W&S strategy was began until April 2018, when PD occurred. Yellow arrows indicate the tumor in cases of PD. The yellow box indicates the post-contrast MRI from May 2015 where the tumor progression was observed. Although radionecrosis was also present, the very high perfusion values (VSRr) indicate a predominant tumor component. The blue box indicates the post-contrast MRI from July 2015, where a major tumor response after bevacizumab can be seen.

Lower row: The patient started a rechallenge with bevacizumab 10 mg/kg/q2wk in April 2018, showing progressive disease as the best response in June 2018 but without clinical deterioration until November 2018, when therapy was stopped and treatment with nivolumab 3 mg/kg/q2wk started. After four cycles, MRI in February 2019 showed progressive disease. Due to concerns of a potential PsPD due to an immune-mediated response, a tumor biopsy was performed that was reported as GB with a very scant T-cell infiltrate (not shown). Given the clinical stability, it was decided to continue nivolumab beyond progression. In May 2019, MRI showed an overt radiologic progression with clinical deterioration (worsening aphasia and gait instability). Treatment with reduced-dose irinotecan (125 mg/m2/q2wk) combined with bevacizumab (10 mg/kg/q2wk) was started with significant toxicity (G2 diarrhea, G3 asthenia) after the first cycle, and the patient and his family decided to definitively stop treatment, being transferred to a palliative-care facility.

BEV, bevacizumab; CNS, central nervous system; CPT-11, irinotecan; CR, complete response; FTM, progressive disease; IDH, isocitrate dehydrogenase; MRI, magnetic resonance imaging; Nivo, nivolumab; PD, progressive disease; PsPD, pseudoprogression; RT, radiotherapy; SD, stable disease; T1 PC, post-contrast T1 image; TMZ, temozolomide; VSRr × 8, perfusion value equivalent to eight times that of the normal-appearing contralateral white matter; W&S, wait and see.

Table 3. Summary of number of TCR clones, Shannon diversity, and Evenness in the biopsies from initial diagnosis in 2013 and that performed in 2019 after four cycles of nivolumab.

	No. of TCR clones	Shannon diversity	Evenness
Tissue pre-nivo (January 2013)	26	3.3997	0.7233
Tissue post-nivo (February 2019)	21	3.0962	0.7049

gliomas treated with anti-PD-1 agents have been reported, demonstrating either objective responses or durable disease control (Table 2).[31–33] To our knowledge, only four other LS-associated gliomas treated with anti-PD-1 agents have been reported to date. In only one of them, the response to single-agent PD-1-inhibition (pembrolizumab) was properly evaluated, showing stable disease as best response and an overall survival of at least 12 months, while the other three reported cases either combined nivolumab with radiotherapy followed by the maintenance nivolumab or used (neo)adjuvant anti-PD-1 agents prior and/or after rescue surgery for newly diagnosed and recurrent GB. Interestingly, two of the latter three cases were alive without disease 20 and 60 months after starting anti-PD-1 therapy (Table 2).[17–19]

Similar to the case reported by Kamiya-Matsuoka *et al.*,[17] our patient did not respond to anti-PD-–1 inhibition, but a slowly progressive disease with a 10-month overall survival was achieved, which suggests a true benefit from nivolumab, given the 9.8-month median OS with nivolumab in second-line recurrent unselected GB patients, while our patient received nivolumab as a sixth line of therapy.[11] Therefore, the heavily treated nature of the tumor of our patient may explain the lack of response and limited survival. The initial biopsy from 2013 and the biopsy performed after four cycles of nivolumab in 2019, however, showed almost complete absence of T cells, thereby suggesting an only minor, at best, antitumor immune response.

We studied the TCR repertoire in the original tumor biopsy from 2013 and the post-nivolumab biopsy from 2019 and found a similar number of T-cell clones, but a completely different T-cell repertoire, with only one T-cell clone being concordant between the two biopsies that significantly increased in the 2019 specimen compared with the prior one from diagnosis. This may be explained because of the high spatial and temporal heterogeneity known to occur in GB, which is a consequence of time and treatment pressure.[34]

We cannot assume that these changes in TCR clonality occurred in response to nivolumab since we could not perform a tumor biopsy immediately prior to the start of anti-PD-1 therapy to make a direct comparison of pre- and post-nivolumab TCR repertoires. Interestingly, other studies have shown that a certain TCR profile may be prognostic in GB patients receiving a personalized antitumor vaccine.[35] In addition, it would have been of interest to study the tumor mutational burden and MSI in our patient's tumor, which, at least in theory, should be TMB-high and MSI-H as it commonly occurs in LS-associated cancers.[18,19,31]

Other heritable syndromes leading to hypermutant cancers that also commonly respond to ICIs are the BMMRDS characterized by the occurrence of gliomas and hematological cancers at early ages, and polymerase deficiency syndrome due to *POL-E* and *POL-D* mutations where both colorectal and endometrial cancers but also gliomas are part of the disease spectrum.[13,14,36] A few cases of gliomas treated with anti-PD-1 agents developed within the BMMRDS and germline *POLE*-mutant syndrome have been reported. Interestingly, responses to PD-1-inhibitors in these BMMRDS-associated gliomas were dramatic and durable in all the four reported cases, suggesting that these pediatric tumors may be specially prone to respond to these agents.[13,15,16] As reported in two of these BMMRD patients, a rapid tumor flare may occur at the start of treatment that should be closely monitored and treated with steroids and anticonvulsants before resuming immunotherapy.[13] Finally, the sole reported case of germline POLE-mutant GB treated with ICIs showed a paradoxical response and developed inflammatory changes after pembrolizumab therapy.[14]

While other immunotherapy modalities, such as CAR-T-cells, vaccines, and oncolytic viral therapy, may be promising in selected patients with gliomas, none of these have been evaluated in gRRD-associated brain tumors, a disease niche where it would be worth evaluating them.[37–41]
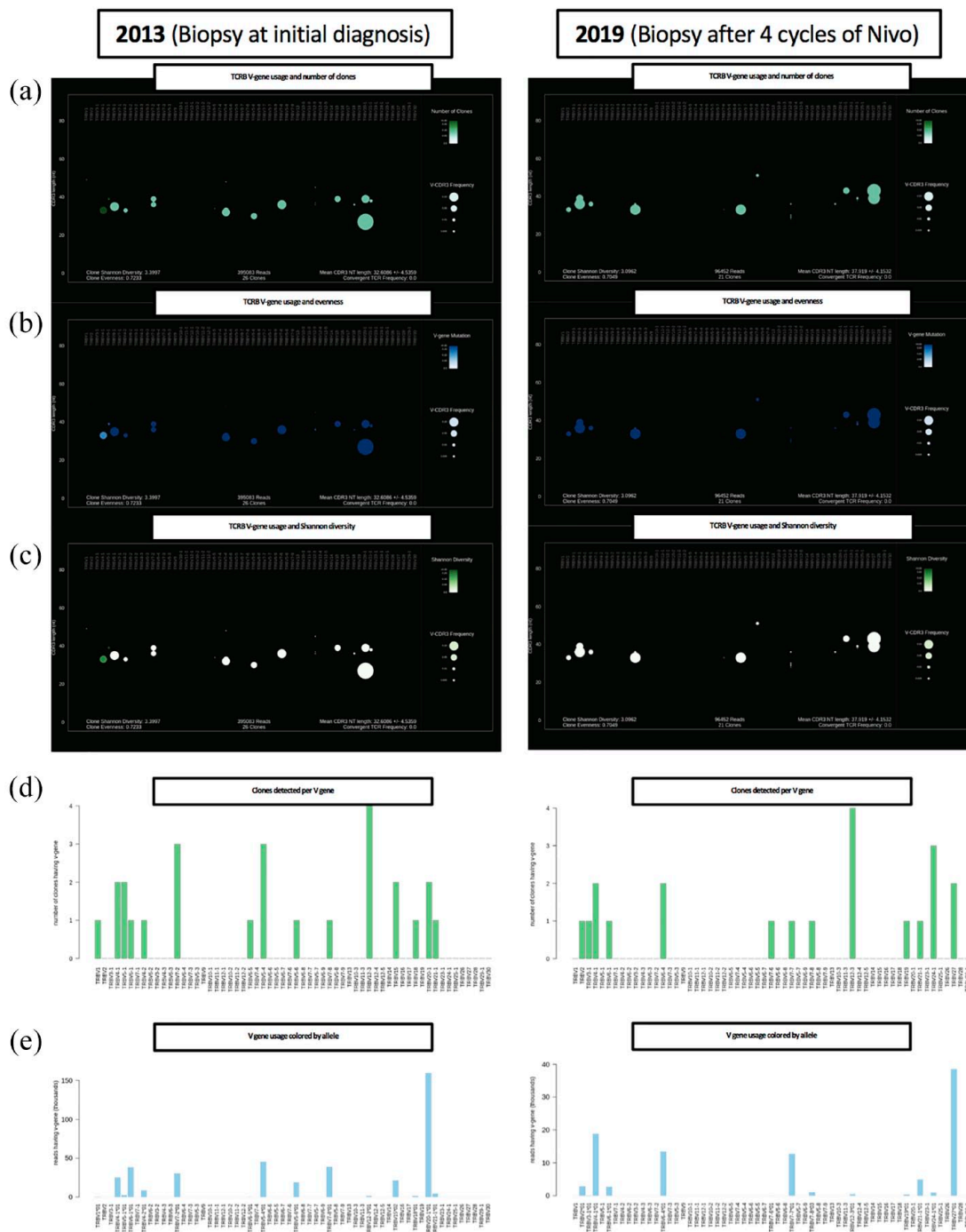
Figure 3. Comparison of the TCR repertoire between the tumor biopsy from initial diagnosis in 2013 and the tumor biopsy performed in February 2019 after four cycles of nivolumab. (a) TCRB V-gene usage and number of T-cell clones. In the 2013 and 2019 biopsies, 26 and 21 clones were identified, respectively. (b) TCRB V-gene usage and evenness. Evenness was 0.7233 and 0.7049 in 2013 and 2019. (c) TCRB V-gene usage and Shannon diversity, the latter achieving 3.3997 and 3.0962 in 2013 and 2019, respectively. (d) Bar plot depicting the number of clones detected per V-gene. (e) Bar plot showing the number of reads per V-gene allele.
TCR, T-cell receptor; V-gene, variable region gene of the TCR.

Our patient experienced an almost 3-year progression-free survival (PFS) after starting bevacizumab in third line which is much longer than the 4.2 months PFS reported in unselected

patients with recurrent GB.[42] While a component of radionecrosis (RN) was present at the time of starting this therapy, and RN is known to be associated with brilliant responses after only four cycles, in our case, there was also a tumoral component as suggested by the very high perfusion values. Therefore, while the near-complete and durable response to bevacizumab may be partially explained by the response of the RN component, the almost 3-year-long response of the tumor component is notable and leads to hypothesize a potential immune-modulatory effect driven by bevacizumab and linked to the MMRd status of the tumor that should be investigated.[43] Indeed, a synergistic effect from anti-PD-1 agents combined with antiangiogenics has been demonstrated in other entities, such as kidney cancer or hepatocellular carcinoma, where both types of agents are commonly used.[44–47] It would have, however, been of interest to study if the tumor belonged to an intrinsic molecular subtype prone to respond to bevacizumab, and other molecular factors related to the angiogenesis process that would explain the response to bevacizumab.[48]

Conclusion

gRRD gliomas are exceptional disease entities that, contrary to sporadic gliomas, seem to benefit from anti-PD-1 therapy. Our case is notable for constituting the fifth LS-associated glioma treated with PD-1-inhibitors. While no response was achieved, a slowly progressive disease was observed and a change in TCR clonality occurred under treatment with nivolumab. Although a rare disease entity, gRRD gliomas could serve as a model to better understand the role of the immune system in the development and treatment of CNS tumors.

ORCID iD

Santiago Cabezas-Camarero [iD] https://orcid.org/0000-0003-4756-7031

Fees from: Merck, MSD and Bristol-Myers Squibb.

Pedro Pérez Segura Consultant for: Bristol-Myers Squibb, Merck, MSD. Speaker's Bureau for: Bristol-Myers Squibb, Merck, MSD. Employee of: None. Grant/Research support from (Clinical Trials): Bristol-Myers Squibb, AstraZeneca, MSD. Travel and Academic work Fees from: Merck, MSD and Bristol-Myers Squibb.

The rest of the authors declare no conflicts of interest relevant to the publication of this article.

Supplemental material

Supplemental material for this article is available online.

References

1. Robert C. A decade of immune-checkpoint inhibitors in cancer therapy. *Nat Commun* 2020; 11: 10–12.

2. Sun L, Zhang L, Yu J, *et al*. Clinical efficacy and safety of anti-PD-1/PD-L1 inhibitors for the treatment of advanced or metastatic cancer: a systematic review and meta-analysis. *Sci Rep* 2020; 10: 1–13.

3. Reiss SN, Yerram P, Modelevsky L, *et al*. Retrospective review of safety and efficacy of programmed cell death-1 inhibitors in refractory high grade gliomas. *J Immunother Cancer* 2017; 5: 1–7.

4. Omuro A, Vlahovic G, Lim M, *et al*. Nivolumab with or without ipilimumab in patients with recurrent glioblastoma: results from exploratory phase I cohorts of CheckMate 143. *Neuro Oncol* 2018; 20: 674–686.

5. Cloughesy TF, Mochizuki AY, Orpilla JR, *et al*. Neoadjuvant anti-PD-1 immunotherapy promotes a survival benefit with intratumoral and systemic immune responses in recurrent glioblastoma. *Nat Med* 2019; 25: 477–486.

6. Zhao J, Chen AX, Gartrell RD, *et al*. Immune and genomic correlates of response to anti-PD-1 immunotherapy in glioblastoma. *Nat Med* 2019; 25: 462–469.

7. Schalper KA, Rodriguez-Ruiz ME, Diez-Valle R, *et al*. Neoadjuvant nivolumab modifies the tumor immune microenvironment in resectable glioblastoma. *Nat Med* 2019; 25: 470–476.

8. Sahebjam S, Forsyth PA, Tran ND, *et al*. Hypofractionated stereotactic re-irradiation with pembrolizumab and bevacizumab in patients with recurrent high-grade gliomas: results from a phase I study. *Neuro Oncol* 2021; 23: 677–686.

9. De Groot J, Penas-Prado M, Alfaro-Munoz K, *et al*. Window-of-opportunity clinical trial of pembrolizumab in patients with recurrent glioblastoma reveals predominance of immune-suppressive macrophages. *Neuro Oncol* 2020; 22: 539–549.

10. Nayak L, Molinaro AM, Peters K, *et al*. Randomized phase II and biomarker study of pembrolizumab plus bevacizumab versus pembrolizumab alone for patients with recurrent glioblastoma. *Clin Cancer Res* 2021; 27: 1048–1057.

11. Reardon DA, Brandes AA, Omuro A, *et al*. Effect of nivolumab vs bevacizumab in patients with recurrent glioblastoma: the checkmate 143 phase 3 randomized clinical trial. *JAMA Oncol* 2020; 6: 1003–1010.

12. Reardon DA, Kim TM, Frenel J-S, *et al*. Treatment with pembrolizumab in programmed death ligand 1-positive recurrent glioblastoma: results from the multicohort phase 1 KEYNOTE-028 trial. *Cancer* 2021; 127: 1620–1629.

13. Bouffet E, Larouche V, Campbell BB, *et al*. Immune checkpoint inhibition for hypermutant glioblastoma multiforme resulting from germline biallelic mismatch repair deficiency. *J Clin Oncol* 2016; 34: 2206–2211.

14. Johanns TM, Miller CA, Dorward IG, *et al*. Immunogenomics of hypermutated glioblastoma: a patient with germline POLE deficiency treated with checkpoint blockade immunotherapy. *Cancer Discov* 2016; 6: 1230–1236.

15. AlHarbi M, Ali Mobark N, AlMubarak L, *et al*. Durable response to nivolumab in a pediatric patient with refractory glioblastoma and constitutional biallelic mismatch repair deficiency. *Oncologist* 2018; 23: 1401–1406.

16. Pavelka Z, Zitterbart K, Nosková H, *et al*. Effective immunotherapy of glioblastoma in an adolescent with constitutional mismatch repair-deficiency syndrome. *Klin Onkol* 2019; 32: 70–74.

17. Kamiya-Matsuoka C, Metrus N, Weathers S, *et al*. *1170 – is immuno-oncology therapy effective in hypermutator glioblastomas with somatic or germline mutations*? *Ann Oncol* 2019; 30(Suppl. 5): v143–v158.

18. Anghileri E, Di Ianni N, Paterra R, *et al*. High tumor mutational burden and T-cell activation are associated with long-term response to

anti-PD1 therapy in Lynch syndrome recurrent glioblastoma patient. *Cancer Immunol Immunother* 2021; 70: 831–842.

19. Sherman WJ and Vitaz TW. Nivolumab with radiation therapy in a glioblastoma patient with Lynch syndrome. *BMJ Case Rep* 2021; 14: 2020–2022.

20. Thomsen W, Maese L, Vagher J, *et al*. Early presentation of homozygous mismatch repair deficient glioblastoma in teen with lynch syndrome: implications for treatment and surveillance. *JCO Precis Oncol* 2021; 5: 670–675.

21. Ahmad H, Fadul CE, Schiff D, *et al*. Checkpoint inhibitor failure in hypermutated and mismatch repair-mutated recurrent high-grade gliomas. *Neurooncol Pract* 2019; 6: 424–427.

22. Lombardi G, Barresi V, Indraccolo S, *et al*. Pembrolizumab activity in recurrent high-grade gliomas with partial or complete loss of mismatch repair protein expression: a monocentric, observational and prospective pilot study. *Cancers (Basel)* 2020; 12: 1–14.

23. Larkin T, Das A, Bianchi V, *et al*. Upfront adjuvant immunotherapy of replication repair–deficient pediatric glioblastoma with chemoradiation-sparing approach. *JCO Precis Oncol* 2021; 5: 1426–1431.

24. Louis DN, Perry A, Wesseling P, *et al*. The 2021 WHO classification of tumors of the central nervous system: a summary. *Neuro Oncol* 2021; 23: 1231–1251.

25. Louis DN, Ohgaki H, Wiestler OD, *et al*. The 2007 WHO classification of tumours of the central nervous system. *Acta Neuropathol* 2007; 114: 97–109.

26. Ravi RK, Walton K and Khosroheidari M. MiSeq: a next generation sequencing platform for genomic analysis. *Methods Mol Biol* 1706: 223–232.

27. Corporation LT. OncomineTM human immune repertoire USER GUIDE [Internet], 2021, https://www.thermofisher.com/document-connect/document-connect.html?url=https%3A%2F%2Fassets.thermofisher.com%2FTFS-Assets%2FLSG%2Fmanuals%2FMAN0017438_OncomineTCRBetaAssay_UG.pdf (accessed 26 March 2022).

28. Kim B, Tabori U and Hawkins C. An update on the CNS manifestations of brain tumor polyposis syndromes. *Acta Neuropathol* 2020; 139: 703–715.

29. Dominguez-Valentin M, Sampson JR, Seppälä TT, *et al*. Cancer risks by gene, age, and gender in 6350 carriers of pathogenic mismatch repair variants: findings from the Prospective Lynch Syndrome Database. *Genet Med* 2020; 22: 15–25.

30. Azam S, Ballester LY, Ramkissoon SH, *et al*. Lynch syndrome with germline MSH2 mutation in a patient with primary anaplastic glioneuronal tumor. *JCO Precis Oncol* 2019; 3: 1–6.

31. Le DT, Durham JN, Smith KN, *et al*. Mismatch repair deficiency predicts response of solid tumors to PD-1 blockade. *Science* 2017; 357: 409–413.

32. Le DT, Uram JN, Wang H, *et al*. PD-1 blockade in tumors with mismatch-repair deficiency. *N Engl J Med* 2015; 372: 2509–2520.

33. Overman MJ, Lonardi S, Wong KYM, *et al*. Durable clinical benefit with nivolumab plus ipilimumab in DNA mismatch repair-deficient/microsatellite instability-high metastatic colorectal cancer. *J Clin Oncol* 2018; 36: 773–779.

34. Miller AM, Shah RH, Pentsova EI, *et al*. Tracking tumour evolution in glioma through liquid biopsies of cerebrospinal fluid. *Nature* 2019; 565: 654–658.

35. Zhang Y, Mudgal P, Wang L, *et al*. T cell receptor repertoire as a prognosis marker for heat shock protein peptide complex-96 vaccine trial against newly diagnosed glioblastoma. *Oncoimmunology* 2020; 9: 1749476.

36. Guerrini-Rousseau L, Varlet P, Colas C, *et al*. Constitutional mismatch repair deficiency–associated brain tumors: report from the European C4CMMRD consortium. *Neurooncol Adv* 2019; 1: vdz033.

37. An Z, Hu Y, Bai Y, *et al*. Antitumor activity of the third generation EphA2 CAR-T cells against glioblastoma is associated with interferon gamma induced PD-L1. *Oncoimmunology* 2021; 10: 1960728.

38. Johanns TM, Miller CA, Liu CJ, *et al*. Detection of neoantigen-specific T cells following a personalized vaccine in a patient with glioblastoma. *Oncoimmunology* 2019; 8: e1561106.

39. Friedman GK, Johnston JM, Bag AK, *et al*. Oncolytic HSV-1 G207 immunovirotherapy for pediatric high-grade gliomas. *N Engl J Med* 2021; 384: 1613–1622.

40. Brown CE, Alizadeh D, Starr R, *et al*. Regression of glioblastoma after chimeric antigen receptor T-cell therapy. *N Engl J Med* 2016; 375: 2561–2569.

41. Platten M, Bunse L and Wick W. Emerging targets for anticancer vaccination: IDH. *ESMO Open* 2021; 6: 100214.

42. Friedman HS, Prados MD, Wen PY, *et al.* Bevacizumab alone and in combination with irinotecan in recurrent glioblastoma. *J Clin Oncol* 2009; 27: 4733–4740.

43. Winter SF, Vaios EJ, Muzikansky A, *et al.* Defining treatment-related adverse effects in patients with glioma: distinctive features of pseudoprogression and treatment-induced necrosis. *Oncologist* 2020; 25: e1221–e1232.

44. Motzer RJ, Penkov K, Haanen J, *et al.* Avelumab plus axitinib versus sunitinib for advanced renal-cell carcinoma. *N Engl J Med* 2019; 380: 1103–1115.

45. Rini BI, Plimack ER, Stus V, *et al.* Pembrolizumab plus axitinib versus sunitinib for advanced renal-cell carcinoma. *N Engl J Med* 2019; 380: 1116–1127.

46. Choueiri TK, Powles T, Burotto M, *et al.* Nivolumab plus cabozantinib versus sunitinib for advanced renal-cell carcinoma. *N Engl J Med* 2021; 384: 829–841.

47. Finn RS, Qin S, Ikeda M, *et al.* Atezolizumab plus bevacizumab in unresectable hepatocellular carcinoma. *N Engl J Med* 2020; 382: 1894–1905.

48. Sandmann T, Bourgon R, Garcia J, *et al.* Patients with proneural glioblastoma may derive overall survival benefit from the addition of bevacizumab to first-line radiotherapy and temozolomide: retrospective analysis of the AVAglio trial. *J Clin Oncol* 2015; 33: 2735–2744.